Quadratic Boost Converter with integrated Energy Storage using PI controller for Low Power Photovoltaic Applications

D. Amudhavalli, Nalin Kant Mohanty

Electrical and Electronics Engineering Department, Sri Venkateswara College of Engineering, Sriperumbudur, Tamil Nadu, India, +919789856567(Email: amudhavalli@svce.ac.in, nkmohanty@svce.ac.in)

Abstract: Quadratic boost converter with integrated energy storage is designed for low power photovoltaic application one among them being DC bus residential PV system. Though the electric power produced by photovoltaic panel provides several advantages like availability of resources for free, maintenance free and long life time, it suffers from intermittent power production, thus creating unstability in power supplied to load. This disadvantage is overcome by integrating a battery in parallel with one of the capacitors of quadratic boost converter. The battery discharges and charges automatically without a separate bi-directional converter, whenever photovoltaic panel power becomes greater than or becomes less than load power, thereby maintaining the power supplied to load constant. Battery discharging and charging transients happen without affecting operation mode of converter. Simplicity, high voltage gain and lesser ripple in input side voltage and current make quadratic boost converter an appropriate converter suitable for photovoltaic applications. A PI controller with inner current controlled loop and outer voltage controlled loop has been designed to obtain voltage regulation at output load side against input side PV panel voltage change with change in insolation. The designed system has been validated with simulation and hardware circuit.

***Keywords**:* Photovoltaic system, Quadratic boost converter, Energy storage, PI controller.

1. INTRODUCTION

The paper introduces a method for interconnecting Photovoltaic panels (PV), electro-chemical energy storage system (EC-ESS) and DC-DC converter in a particular way that self-balances power supplied to load. In specific, quadratic boost DC-DC converter (QBC) with integrated EC-ESS is designed to eliminate fluctuation of PV power reaching load. This avoids a separate DC-DC converter and complex control circuits involved in discharging/charging EC-ESS.

Interest to the design of such circuit was motivated by exponential growth in the use of photovoltaic system in distributed generation due to its advantages like free of cost, long life time and maintenance free. Intermittencies in power production with changing insolation necessitated cost effective self charging design for PV and EC-ESS.

Achieving 100% Renewable Grid is not possible without the high level of penetration of Photo voltaic system (Kroposki et al., 2017). Decrease in the cost of this technology over last few years has contributed large-scale deployments of PV panels around world. Photovoltaic systems though are intermittent but are sustainable energy sources. Establishment of PV system and integrating to grid might not have become popular due to variation in power produced with varying insolation (Moumouni et al., 2014). However this is overcome by connecting Battery Energy Storage system that stores excess PV power and provide power to load when PV power is insufficient for load. Energy storage system should be established to achieve constant power production in PV panel (Beltran et al., 2013). Hence, energy storage becomes a key issue for integrating PV panel to grid.

This paper mainly develops QBC with integrated energy storage suitable for Low Power Residential systems. Most of the residential electrical loads internally requires DC voltage for its working, that is obtained by stepping down rectified AC voltage supply (Manandhar et al., 2015). Photovoltaic panels are capable of producing this DC voltage at low voltage value [Jagadish Kumar Patra., et al, 2016]. Therefore rectification of AC to DC power could be eliminated. DC voltage when used from isolated micro grids provides substantial efficiency improvement and potential for reduction in cost in all cases is promising (Rodriguez-Diaz et al., 2015; Wunder et al., 2014). DC micro grid also have advantages like high reliability, no reactive power issues, lack of frequency and simple connection to PV panels. PV power generation is an ideal system of power generation that generates electricity directly from sunlight. Since the power handled is only active power, size of wiring and DC link capacitors are reduced. Their applications also include residential building, islanded power supplies, data centres, communication systems, metro train and electric vehicles.

However distribution of regulated power supply has several practical challenges (Li et al., 2012). DC micro grid when supplied with low voltage and high current it requires high gauge cables, leading to increase in overall losses (Starke et al., 2008). To reduce this loss and save initial cost of installation, DC micro-grid voltage should have large value. Research works have been made to reduce spark phenomenon and arcing in order to enhance DC distribution system. However, the paper deals with loads not requiring more than 240 V.

Traditionally in development of photovoltaic system, bi-directional converters have been playing a vital role in discharge/charge regulation of EC-ESS (Jadhav et al., 2018). Generally DC grid powers downstream load converters and bidirectional converter operates in boost/buck mode to discharge/charge battery (Dong et al., 2012).

A solution was addressed in literature (Ge et al., 2018). Battery energy storage system was connected in parallel to one of the capacitors of Quasi Z source inverter; by this way discharge/charge regulation was done automatically eliminating a separate DC–DC converter usually employed for EC-ESS (Ge et al., 2014). The system was complex since many objectives like increasing voltage gain and DC – AC power inversion were achieved using a single inverter circuit by adjusting shoot through duty ratio. Table. 1 shown further discusses necessary of energy storage in PV systems followed by use of bidirectional converter for discharge/charge of battery. Table.1 also continues with suggestion for cost reduction techniques applied in PV systems.

Table 1. Extended Literature survey.

Author Name	Characteristic addressed for	System Description
Vieira et al., 2017	EC-ESS	ESS for residential buildings in PV system is proposed. A control system minimized the costs of energy bills to 87.2% making cost-effective before 2020.
Nyholm et al., 2016	EC-ESS	A model with batteries in household PV systems was developed. The batteries used increased self-consumption of electricity by 20–50%.
Ren., 2016	EC-ESS	Adoption of PV battery systems, incurred greatest savings in households at critical peak pricing retail energy and network capacity charge.
Child et al., 2019	EC-ESS	Two transition pathways featuring 100% renewable energy were simulated for Europe. Grid interconnection and use of PV with Energy storage System is considered to be a super smart approach.
Gulagi et al., 2018	EC-ESS	100% Renewable energy system is again assured only with the help of storage technologies. New inventions made in the material of storage batteries like Lithium-carbon-dioxide battery, creates opportunities like extension made in life, fast discharging/charging of batteries, cost reduction and high operating temperature urges to use storage batteries for energy storage throughout the globe.
Metwally et al., 2019	Bidirectional converter	Bidirectional converters are a power converter that transfers power in both directions. They were used at first to discharge/charge batteries in spacecraft applications. Then their application extended to Energy recovery systems based in super capacitors for elevators, cranes, and other braking applications such as for trains or roller coasters, Electric and hybrid vehicles, UPS systems, smart Grids, Vehicle2-Grid, hybridize different types of batteries and super capacitors to extend life expectancy and reduce overall costs of energy storage systems.
Haroun et al., 2018	Bidirectional converter	Bidirectional Dual Active Bridge converter is used for electric vehicle battery charging.
Silveira et al., 2018	Bidirectional converter	A comparative evaluation of different converter topologies of bidirectional (DC-DC) converter is made in hybrid micro grids with Photovoltaic and Battery Technologies. A topology with high voltage regulation is designed.
Kavya Santhoshi et al., 2020	Single stage converter	Cost effective single stage converters was proposed.
Ge et al., 2012	Single stage converter	These single stage converters are capable of buck-boost operation of voltage by varying shoot through duty cycle. They convert DC power available from PV to AC power in single stage using Quasi–Z-source inverter. Integration of battery storage i.e. battery is connected in parallel with one of the capacitors of QZSI, enables in stabilizing power supplied to load by discharging/charging. Hence separate bidirectional converters generally employed for discharging/charging of battery was eliminated, ensuring cost reduction of PV system and reduction of microcontrollers employed in controlling the bidirectional converters.
Liu et al., 2013	Single stage converter	Energy storage device integrated with QZSI needed no extra circuit for charging. Operation is grouped in to two modes, first mode in low PV power mode, where battery is discharged and second mode in high power mode, where battery is charged. Hence, extended PV power operating range is achieved where lack of its power can be supported with power of battery.
Liu et al., 2014	Single stage converter	Quasi Z source inverter with battery based photovoltaic power system is modelled. Controller proposed enhances maximum power tracking, battery management system and achieves unity power factor.
Liang et al., 2017	Single stage converter	Degradation made in single stage power processing by second harmonic power ripple was eliminated with the design of impedance model for QZSI.

Khajesalehi et al., 2015	Single stage converter	Single-stage grid-connected photovoltaic (PV) module-integrated converter (MIC) based on cascaded quasi-Z-source inverters (qZSI) presented to feature low voltage gain requirement enhanced reliability and better output power quality.
Lopes et al., 2016	Cost reduction technique	Load matching improvement in individual buildings was made by introducing Cooperative Net Zero Energy Community using demand side management method using genetic algorithm. This increased onsite electricity generation to 15%.
Nottrott et al., 2013	Cost reduction technique	Optimization method for demand charge management of photovoltaic-battery systems was proposed. Application of PV and load forecasts increased the net present value of the battery, decreasing cost of battery by 40 – 50% compared to year 2011.
Bortolini et al., 2014	Cost reduction technique	Model to manage energy flow and determine system profitability is presented. It also evaluates effective PV power rate and battery energy system capacity.

The paper proposes a simple topology of QBC with EC-ESS that overcomes fluctuations in solar power and supply constant power to load suitable for low power photovoltaic application. Discharge/Charge transitions of energy storage system are automatically made with respect to fluctuation in PV panel and load power, thereby eliminating the need for a bi-directional DC – DC converter. The energy stored quadratic boost converter (ES-QBC) simultaneously

A) Supplies constant power to load irrespective of variations in input solar power.
B) It also regulates Charge state of battery automatically without the need of a bi-directional converter.

Section 2 describes the operation modes of simple model proposed for low power application. The operation of DC – DC converter does not affect discharge/charge regulation of EC-ESS. It happens independently without affecting operation mode of circuit. Development of a closed loop using PI controller with inner current controller and outer voltage controller for voltage regulation at load end is discussed in section 3. Simulation of proposed system has been presented in section 4. Section 5 provides experimental validation of system proposed. Lastly, section 6 concludes this report with a summary.

2. OPERATION MODE

In first section, operation of a simple model is discussed to provide clear understanding of concept proposed.

2.1 Working of Simple Model

Figure. 1 shows the conventional QBC. This converter is a promising high gain converter that is likely to gain popularity in future. It comprises of two LC filters and is classified under fourth order DC – DC converter. It consist of a single switch S, two inductors L_1 and L_2, two capacitors C_1 and C_2 and three diodes D_1, D_2, and D_0. Vg denotes input photovoltaic panel DC voltage, R_L represents load resistance and V_0 stands for output voltage of converter. Stochastic fluctuations of the power present in photovoltaic panel necessitate the battery storage.

Battery should be in the charging mode when the photovoltaic power exceeds load demand and it has to be in discharging mode as the photovoltaic power becomes lesser than load demands. Figure 2 shows the proposed ESQBC. Battery connected in parallel with capacitor C_1, automatically charges when the photovoltaic power becomes greater than load demands and discharges when the photovoltaic power becomes lesser than load demands. Discharging and charging of the battery happens only with respect to the power balancing between the panel and the load and does not affect the modes of operation of the QBC considered for the step-up operation.

Power equation governing the proposed circuit is

$$P_{in} - P_{out} + P_{bat} = 0 \tag{1}$$

where, P_{in} represents the power from the photovoltaic panel, P_{out} represents the power that is delivered to load side and P_{bat} represents power of the battery connected in parallel with capacitor C_1.

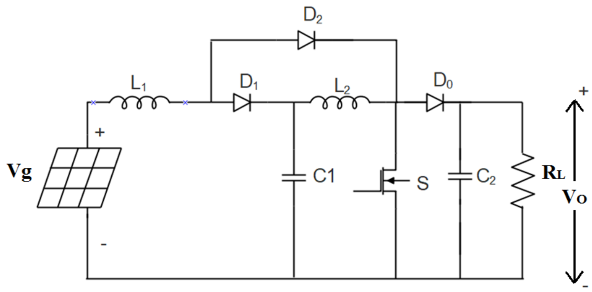

Fig. 1. Conventional Quadratic Boost Converter.

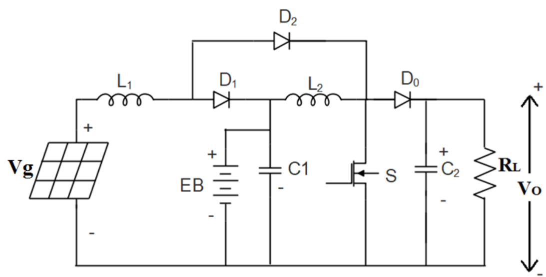

Fig. 2. Quadratic Boost Converter with Energy storage.

Power from panel remains always positive, since it is unidirectional. Output power is positive when power flows through the converter to load side and battery power is positive when it discharges power to load side and is considered negative when it charges power from panel. As the two powers are balanced, third power is balanced automatically.

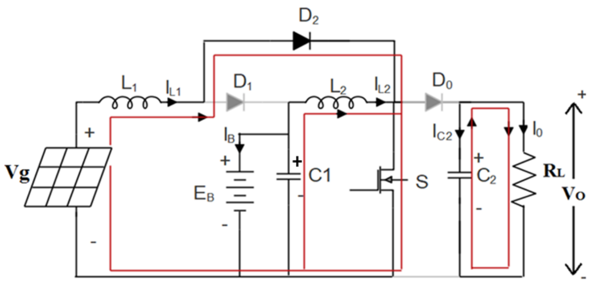

Fig. 3. Mode 1 Operation of proposed quadratic boost converter.

Figure 3 shows mode 1 operation of the QBC where the red curls represent direction of current flowing in converter. In this mode switch S turns on. Inductor L_1 is charged from the photo-voltaic panel through current path V_g, L_1, D_2 and S and L_2 is charged from the charge stored in capacitor C_1, through current path C_1, L_2 and S and the load current through load resistance is maintained by charge stored in capacitor C_2. Steady state equations are obtained by applying Kirchhoff's voltage law and current law across the two inductors L_1, L_2 and the two capacitors C_1, C_2. The equations are given below.

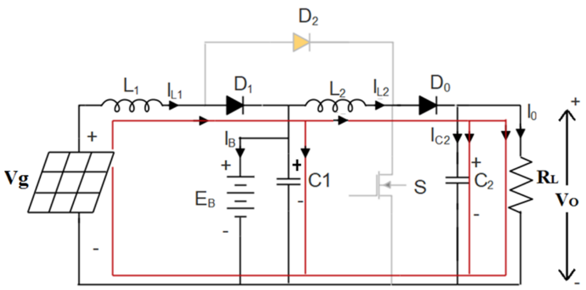

Fig. 4. Mode 2 Operation of proposed quadratic boost converter

$$\frac{di_{L1}}{dt} = \frac{V_g}{L_1} \quad (2)$$

$$\frac{di_{L2}}{dt} = \frac{V_{C1}}{L_2} \quad (3)$$

$$\frac{dV_{C1}}{dt} = \frac{i_{L2}}{C_1} - \frac{i_{bat}}{C_1} \quad (4)$$

$$\frac{dV_{C2}}{dt} = \frac{V_{C2}}{R_0 C_2} \quad (5)$$

Figure 4 shows mode 2 operation of the QBC. In this mode switch S turns off, inductors L_1 and L_2 discharge their stored energy to the load. Hence the current from photo-voltaic panel flows through inductor L_1, through diode D_1 and charges capacitor C_1, as shown by the red curls. Simultaneously, the current from photo-voltaic panel flows through discharging inductor L_1, L_2, diode D_0 and to the load, as shown by the red curls. Steady state equations for mode 2 operation of converter are given below.

$$\frac{di_{L1}}{dt} = \frac{V_g - V_{C1}}{L_1} \quad (6)$$

$$\frac{di_{L2}}{dt} = \frac{V_{C1} - V_{C2}}{L_2} \quad (7)$$

$$\frac{dV_{C1}}{dt} = -\frac{i_{L1}}{C_1} + \frac{i_{L2}}{C_1} - \frac{I_{bat}}{C_1} \quad (8)$$

$$\frac{dV_{C2}}{dt} = \frac{i_{L2}}{C_2} - \frac{V_{C2}}{R_0 C_2} \quad (9)$$

The battery paralleled with capacitor makes the circuit work in a different way, no more magnitude of inductor current, I_{L2} remains the same during discharge/charge transitions of battery and capacitor voltage is clamped to battery voltage. Suitable closed loop control is designed with inner current loop and outer voltage loop using PI controller to maintain output voltage constant irrespective of input voltage variations.

Applying a volt – sec balance on the inductors L_1, L_2 produces (10) and (11),

$$\int_0^{dT} V_g \, dt + \int_{dT}^{T} (V_g - V_{C1}) \, dt = 0 \quad (10)$$

$$\int_0^{dT} V_{C1} \, dt + \int_{dT}^{T} (V_{C1} - V_0) \, dt = 0 \quad (11)$$

Solving equation (10) and (11) yields (12) and (13)

$$V_{C1} = \frac{V_g}{(1-d)} \quad (12)$$

$$V_0 = \frac{V_{C1}}{(1-d)} \quad (13)$$

Substituting (12) in (13) obtains the gain of QBC

$$V_0 = \frac{V_g}{(1-d)^2} \quad (14)$$

Inductor current peak to peak relation is obtained from (2) and (3)

$$\Delta i_{L1}(dT) = \frac{V_g dT}{L_1} = \frac{V_g d}{L_1 f} \quad (15)$$

Hence

$$L_1 = \frac{V_g d}{\Delta i_{L1} f} \quad (16)$$

$$\Delta i_{L2}(dT) = \frac{V_{C1} dT}{L_2} = \frac{V_{C1} d}{L_2 f} \quad (17)$$

Substituting (12) in (17), we get

$$\Delta i_{L2}(dT) = \frac{V_g d}{(1-d) L_2 f} \quad (18)$$

Hence

$$L_2 = \frac{V_g d}{\Delta i_{L2} f (1-d)} \quad (19)$$

Considering rate of charge stored in capacitance,

$$\Delta Q_1 = C_1 \Delta V_{C1} = I_{L2} dT \quad (20)$$

$$\Delta Q_2 = C_2 \Delta V_{C2} = I_0 dT \quad (21)$$

Transposition of the above two equations yields capacitance equation

$$C_1 = \frac{I_0 d}{(1-d)\Delta V_{C1} f_s} \tag{22}$$

$$C_2 = \frac{I_0 d}{\Delta V_{C2} f_s} \tag{23}$$

3. STATE SPACE MODEL

State space analysis is made for the simple model proposed. This examines transient behaviour of converter (Leyva-Ramos et al., 2017). Using (2) to (9) state space equations are obtained.

Here the state variables assumed are $x = [x_1, x_2, x_3, x_4]^T = [I_{L1}, I_{L2}, V_{C1}, V_{C2}]^T$.

State space equation when switch S turns on is given by

$$\begin{bmatrix} \dot{x}_1 \\ \dot{x}_2 \\ \dot{x}_3 \\ \dot{x}_4 \end{bmatrix} = \begin{bmatrix} 0 & 0 & 0 & 0 \\ 0 & 0 & \frac{1}{L_2} & 0 \\ 0 & -\frac{1}{C_1} & 0 & 0 \\ 0 & 0 & 0 & -\frac{1}{R_0 C_2} \end{bmatrix} \begin{bmatrix} x_1 \\ x_2 \\ x_3 \\ x_4 \end{bmatrix} + \begin{bmatrix} \frac{1}{L_1} & 0 \\ 0 & 0 \\ 0 & -\frac{1}{C_1} \\ 0 & 0 \end{bmatrix} \begin{bmatrix} V_g \\ i_{bat} \end{bmatrix} \tag{24}$$

State space equation when switch S turns off is given by

$$\begin{bmatrix} \dot{x}_1 \\ \dot{x}_2 \\ \dot{x}_3 \\ \dot{x}_4 \end{bmatrix} = \begin{bmatrix} 0 & 0 & -\frac{1}{L_1} & 0 \\ 0 & 0 & \frac{1}{L_2} & -\frac{1}{L_2} \\ \frac{1}{C_1} & -\frac{1}{C_1} & 0 & 0 \\ 0 & \frac{1}{C_2} & 0 & -\frac{1}{R_0 C_2} \end{bmatrix} \begin{bmatrix} x_1 \\ x_2 \\ x_3 \\ x_4 \end{bmatrix} + \begin{bmatrix} \frac{1}{L_1} & 0 \\ 0 & 0 \\ 0 & -\frac{1}{C_1} \\ 0 & 0 \end{bmatrix} \begin{bmatrix} V_g \\ i_{bat} \end{bmatrix} \tag{25}$$

By applying state space average to (24) and (25), we obtain the average model, as obtained in (26).

$$\begin{bmatrix} \dot{x}_1 \\ \dot{x}_2 \\ \dot{x}_3 \\ \dot{x}_4 \end{bmatrix} = \begin{bmatrix} 0 & 0 & -\frac{(1-D)}{L_1} & 0 \\ 0 & 0 & \frac{1}{L_2} & -\frac{(1-D)}{L_2} \\ \frac{(1-D)}{C_1} & -\frac{1}{C_1} & 0 & 0 \\ 0 & \frac{(1-D)}{C_2} & 0 & -\frac{1}{R_0 C_2} \end{bmatrix} \begin{bmatrix} x_1 \\ x_2 \\ x_3 \\ x_4 \end{bmatrix} + \begin{bmatrix} \frac{1}{L_1} & 0 \\ 0 & 0 \\ 0 & -\frac{1}{C_1} \\ 0 & 0 \end{bmatrix} \begin{bmatrix} V_g \\ i_{bat} \end{bmatrix} \tag{26}$$

For control purpose, it is essential to select variable that are appropriate for performance and implementation. In this converter, the selected state variables correspond to inductor currents and capacitor voltages. By considering (26) transfer functions are derived with following characteristics (Leyva-Ramos et al., 2009): $i_{L1}(s)/d(s)$, corresponds to stable and minimum phase, and $i_{L2}(s)/d(s)$, $V_{C1}(s)/d(s)$ and $V_{C2}(s)/d(s)$ correspond to stable and non-minimum phase. It is known that for conventional boost converter $V_0(s)/d(s)$ is a non-minimum phase transfer function, that has right half side zeros. In the case of this class of cascaded boost converter, all transfer functions $i_{L2}(s)/d(s)$, $V_{C1}(s)/d(s)$ and $V_{C2}(s)/d(s)$ exhibits same characteristics except $i_{L1}(s)/d(s)$. Hence, in this paper the inductor current i_{L1} is measured for control. The transfer function of $i_{L1}(s)/d(s)$ is given by

$$\frac{i_{L1}(s)}{d(s)} = k_1 \frac{s^3 + a_2 s^2 + a_1 s + a_0}{s^4 + b_3 s^3 + b_2 s^2 + b_1 s + b_0} \tag{27}$$

The transfer function of $V_0(s)/d(s)$ is given by

$$\frac{V_0(s)}{d(s)} = k_2 \frac{s^3 + m_2 s^2 + m_1 s + m_0}{s^4 + b_3 s^3 + b_2 s^2 + b_1 s + b_0} \tag{28}$$

The expressions for coefficients a_0, a_1, a_2, b_3, b_2, b_1, b_0, m_2, m_1 and m_0 could be found in paper (Leyva-Ramos et al., 2009).

Depending on the power obtained from the photo-voltaic panel, three different operation modes can be classified as given in the Table. 2.

Table. 2 Relationships between P_{in}, P_0, and P_{bat}.

Input and Output power relationship	Battery Power
$P_{in} < P_0$	$P_{bat} > 0$, Discharging state
$P_{in} > P_0$	$P_{bat} < 0$, Charging state
$P_{in} = P_0$	$P_{bat} = 0$, Floating state

As given in Table.2 three different situations happen due to the stochastic fluctuation of the photo-voltaic power with the variation of insolation, here depending upon the power difference happening between the source and load power, the behaviour of the discharge and charge mode of the integrated energy storage, the operation of the circuit is classified into three different cases, where in the first case photo-voltaic power is lesser than the load demand, in the second case photo-voltaic power becomes greater that load demand and in the third case photo-voltaic power becomes equal to the load demand.

4. SIMULATION AND RESULTS DISCUSSION

The proposed circuit comprising of photo-voltaic panel, QBC, battery, and load resistance is simulated using MATLAB / Simulink software and is indicated in Figure 5 QBC is designed for power rating of 2500 W. By applying design equations at a switching frequency of 5000 Hz, values of inductor L_1, L_2 has been calculated to be 0.383 mH, 2.66 mH, C_1 and C_2 has been calculated to be 100 μF respectively. Battery is considered for 7 Ah, 90 V with a charge state of 85 %. The nominal load is 23 Ω. Circuit parameters for the simulation of the designed circuit are shown in Table. 3.

Substituting the values of V_g, L_1, L_2, C_1, C_2 and duty cycle, d the value of coefficients a_0, a_1, a_2, b_3, b_2, b_1, b_0, m_2, m_1 and m_0 present in (27) and (28) could be found. Hence the transfer function for $i_{L1}(s)/d(s)$ is calculated and expressed in (29).

Table. 3 Parameters of ESQBC.

Parameters	Values
Input power	Case i: 3000 W, Case ii: 2000 W
Battery Power	7 Ah
Output Power	2500 W
Input Voltage, V_{in}	Case i: 50 V, Case ii: 45 V
Output Voltage, V_0	240 V
Capacitor, C_1	100 µF
Capacitor, C_2	100 µF
Inductor, L_1	0.383 mH
Inductor, L_2	2.66 mH
Switching Frequency, f_s	5000 Hz
Load resistance, R_0	23 Ω

$$\frac{i_{L1}(s)}{d(s)} = 261096.6\ \frac{s^3+2173.8s^2+29891481.5s+6538084341}{s^4+437.78s^3+11226657.64s^2+4472527669s+6.134788e12} \tag{29}$$

Hence the transfer function for $V_0(s)/d(s)$ is calculated and expressed in (30).

$$\frac{V_0(s)}{d(s)} = -173913\ \frac{s^3-2161.65s^2+14046212s+1.1288e11}{s^4+437.78s^3+11226657.64s^2+4472527669s+6.134788e12} \tag{30}$$

The QBC has fourth order dynamics behaviour due to the presence of second order filter, that have high quality factor Q, that depends on converter parameters. Here, the transfer function $V_0(s)/d(s)$ exhibits dynamics related to fourth order and non-minimum phase. This transfer function has one zero in left half of s-plane and two zeros located in the right half of s-plane {-3413, 2787.4 ± j 5030.3} and poles at {-8.9 ± j 3262.3, -209.6 ± j729.7}.

There are high resonant peaks that depend on converter parameters. A good closed loop performance is very difficult to achieve with a single control loop. Hence, the control is implemented with inner current control, sensing i_{L1} that has zeros and poles in the left half of s-plane. In this paper control is implemented by measuring inductor current i_{L1} for feedback purpose together with output voltage. PI controller in both loops is tuned using Zeigler Nichol's method of tuning.

Since the PV system is proposed for Residential application, design of low cost and physically realisable system that could be put to practice is most preferred. Values of the proportional constant K_p and the integral constant K_i are obtained by Zeigler Nichols tuning method, for the outer loop they are chosen as 1 and 0.01 respectively, while for the inner loop they are taken to be 1.2 and 0.05.

As the insolation of photo-voltaic panel varies, power generated by photo-voltaic panel varies; additionally its terminal voltage also varies. Consequently, discharging/charging of the battery voltage changes with the change in percentage charge state of the battery. However, use of current controller overcomes the variation in magnitude of the load terminal voltage and maintains its constancy at 240 V.

In the first case, panel power is maintained at 3000 W. As the photo-voltaic power becomes greater than load demands, excess power is stored in the battery. In the second case, panel power is reduced to 2000 W, as this power is lesser than load demands, battery supplies power of 500 W and maintains output power to 2500 W. In both cases power supplied to load remains constant.

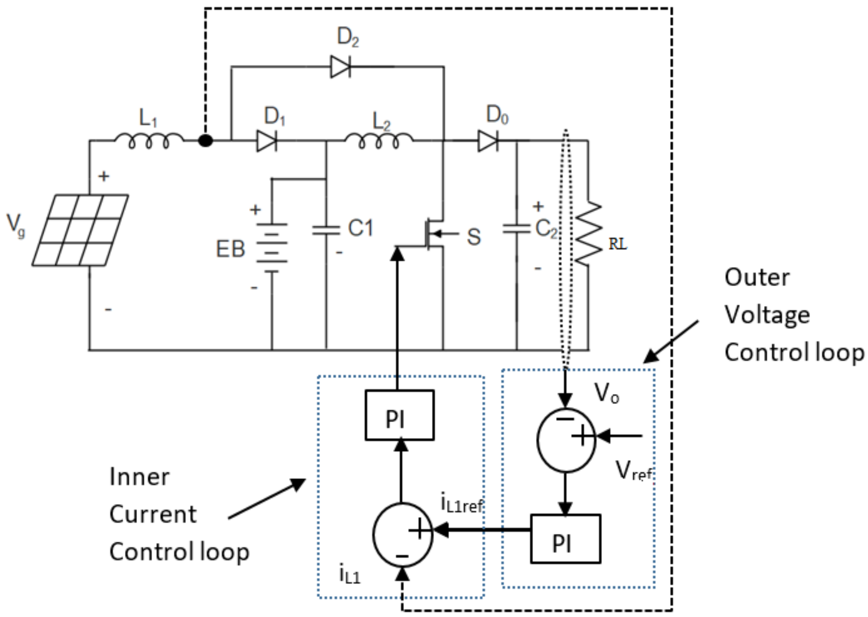

Fig. 5. Simulation circuit for closed loop system of ESQBC.

Simulation of the designed circuit has been made in MATLAB/Simulink and input waveforms for input power P_{in}, input voltage V_{in}, input current i_{in}, and output waveforms for output power P_0, output voltage V_0, output current i_0

between two stages (stage I: when photo-voltaic power becomes greater than load demands. Stage II: when photo-voltaic power is lesser than load demands) are shown in Figure. 6 to Figure. 8.

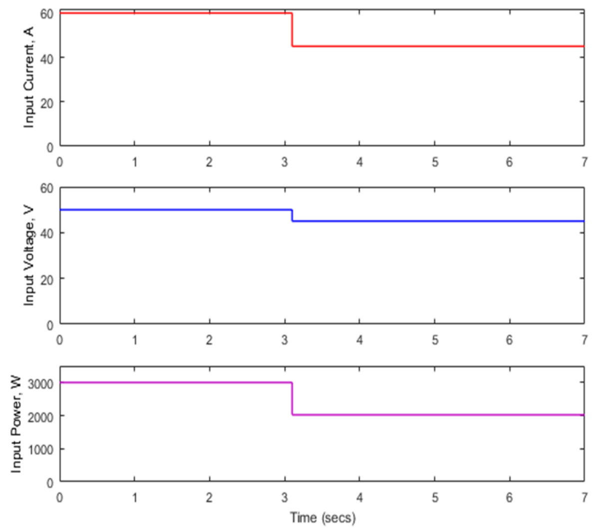

Fig. 6. Comparison waveform for input power P_{in}, input voltage V_{in}, input current i_{in}, between two stages (Case i: when photo-voltaic power becomes greater than load demands. Case ii: when photo-voltaic power is lesser than load demands).

From the initial time to 3 seconds photo-voltaic panel power is maintained at 3000 W, 50 V, and 60 A at an insolation of 1000 W/m^2 and for the same time output power at load is 2500 W with voltage at 240 V and load current of 10.416 A.

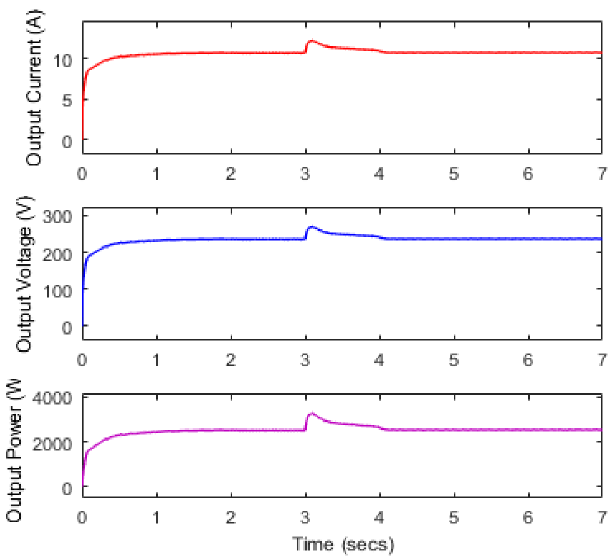

Fig. 7. Comparison waveform for output power P_0, output voltage V_0, output current i_0, between two stages (stage I: when photo-voltaic power becomes greater than load demands. Stage II: when photo-voltaic power is lesser than load demands).

At this stage since the input power becomes greater than load power, battery starts to charge the excess power of 500 W available from panel which is shown by the charging battery current $-I_{bat}$ in Figure.8. When insolation of photo-voltaic panel is brought down to 700 W/m^2 as shown by Figure. 6 to Figure 8 from 3 secs to 7 secs, photo-voltaic panel power reduces to 2000 W, with input voltage becoming 45 V, and current to 40 A as shown by Figure. 6. Now output power at the load is automatically maintained constant as 2500 W, by the discharging battery current I_{bat}, but output voltage fluctuates with respect to the fluctuation in input voltage. This can be overcome with the designed PI controller having inner current and outer voltage loop to maintain constant output voltage. However, a transition time of 1 second is required for the output power P_0, output voltage V_0, output current i_0 waveforms to settle down to their new final values which can be confirmed from Figure. 7 from 3 secs to 4 secs.

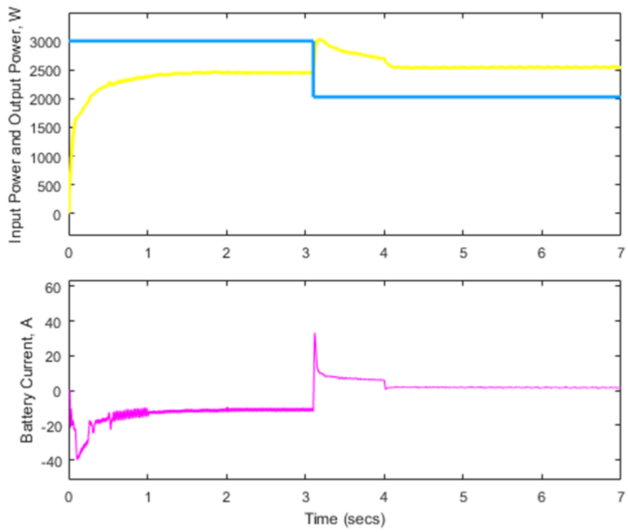

Fig. 8. Comparison waveform for output power P_0, input power P_{in}, battery current I_B, between two stages (stage I: when photo-voltaic power becomes greater than load demands. Stage II: when photo-voltaic power is lesser than load demands).

The automatic discharging/charging of ESQBC happens in the same manner as suggested by (Ge et al., 2014; Liu et al., 2013) in literature, the authors have experimented this automatic discharging/charging concept in quazi Z source inverter integrated with battery. This converter is a DC-AC converter that converts DC power of PV panel to AC power; such converters are only suitable for transmitting PV panel power to either grid or AC load. Such converters are no-way suitable for Residential home that uses DC grid and DC loads. But quadratic boost converter is a suitable converter with advantages like high gain, single switch and a DC-DC converter, that is capable of boosting PV power available at low voltage to a high voltage level that is suitable for DC bus voltage fixed for a Residential home especially with DC loads that exploits DC power of PV panel in an efficient way with less losses compared to other topologies that converts DC power of panel to AC and again converts to DC and feed DC loads. Integration of integrated energy storage into this converter stabilizes power reaching DC grid with elimination of bi-directional converter reducing complexity involved in controlling bi-directional converter, reducing size, volume and cost of power electronic interfacing circuits involved in processing PV power.

Figure. 8 depicts comparison waveforms of output power P_0, input power P_{in} and battery current I_{bat} between two stages. It can be understood that the output power remains stable and constant even when the input photo-voltaic power is varied, but a transition time of 1 second is required for the output power to settle to its new value. Thus the battery connected in parallel with capacitor C_1 of proposed QBC, automatically reacts to overcome the fluctuations of power and voltage at the input side without using a bi-directional DC – DC converter. This provides advantages like

i) Reducing the cost of the designed system with cancellation of bi-directional switch.
ii) Exclusion of separate microcontroller for the control of bi-directional switch, thereby reducing the complexity of system.

Figure. 9 represents percentage state of the charge of the battery %SOC, battery current I_{bat} and battery voltage V_{bat}. From zero to 3 seconds when the input power becomes greater than load demands, charging of battery is illustrated by charge rising linearly from 83.35 % to 83.50 %. As shown by Figure.9 charging battery current is represented with negative polarity and battery voltage rises slowly. As input power becomes lesser than load demands, battery discharges, because of this percentage state of the charge of the battery slowly reduces, thereby reducing battery voltage. From Figure 9 it is proved that battery voltage varies with respect to the discharging and charging of battery, thereby altering the load voltage.

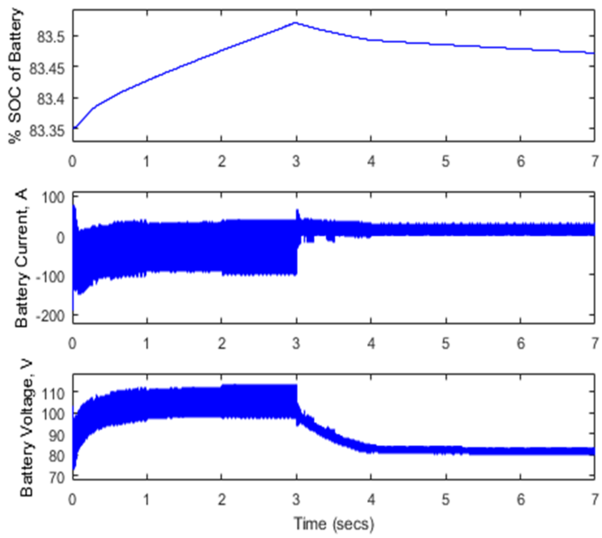

Fig. 9. Comparison waveform for percentage state of the charge of the battery %SOC, battery current I_{bat} and battery voltage V_{bat} between two stages (stage I: when photo-voltaic power becomes greater than load demand. Stage II: when photo-voltaic power is less than load demand).

This necessitated for the design of suitable PI controller that was capable of eliminating transition of voltage fluctuation from input side to output load side. PI controller is cost effective compared to other converters. They also hold advantages like less computational burden, occupancy of less memory, easily applicable in practice with selection of low switching frequency and have easy design process. Integrated energy storage proposed in this paper mainly reduces entire cost of designed PV system. Hence to make entire system cost effective, simple PI controller is suggested for closed loop control. Comparison made with Figure. 6 and 7 proves how input voltage fluctuations are eliminated in output voltage with the help of PI controller.

5. EXPERIMENTAL ANALYSIS

A laboratory prototype was built to validate the proposed ESQBC. The photograph of the experimental prototype is given in Figure. 10. It consist of QBC, input source, lead acid battery bank, voltage and current sensors, PIC microcontroller PIC16f877a, opto-couplers and voltage regulators that supply +5V to the PIC microcontroller. This system demonstrates that the QBC is capable of maintaining charge state of the battery connected in parallel with the capacitor and also is capable of precluding the power fluctuation present at the load side with the variation in the photo-voltaic power.

In hardware PV panel is replaced by switched mode regulator with variable resistor to obtain preliminary characteristics of PV panel (Lopes et al., 2003). It is operated for two different input voltages to illustrate variation in PV panel power with change in insolation. Two input voltages are 11 V and 14 V. The parameters are $L_1 = L_2 = 1$mH, $C_1 = C_2 = 100$ µF, battery voltage is 24 V and load resistance is 25 Ω. A digital oscilloscope TS2024B with voltage probes HP3060 and Tektronix A622 AC/DC current probe from TEKTRONIX was used to measure the hardware waveforms.

A battery is connected in parallel with the capacitor of the QBC through a breaker, which is controlled by embedded system through driver. When the source voltage is low, battery starts to discharge and when the source voltage is high, battery starts to charge in parallel with the capacitor. The voltage status of battery is monitored by Signal Conditioning Unit. Embedded system is programmed to disconnect the Battery from the converter when input voltage of converter and the battery voltage are both low.

For testing two operating modes are considered:

1. Photo-voltaic power is more than load demands; hence battery is in the charging mode.
2. Photo-voltaic power is lesser than load demands; hence battery is in discharging mode.

Figure. 11 shows waveform for discharging and figure.12 shows waveforms for charging of battery. Terminal voltage of PV is generally lower when it generates lesser power at less insolation and it is slightly higher when it generates more power at higher insolation. When input voltage is 10.5 V, the battery enters discharging state. Figure 11 (a) shows input voltage V_{in}, output voltage V_{out} and battery current I_{bat}.

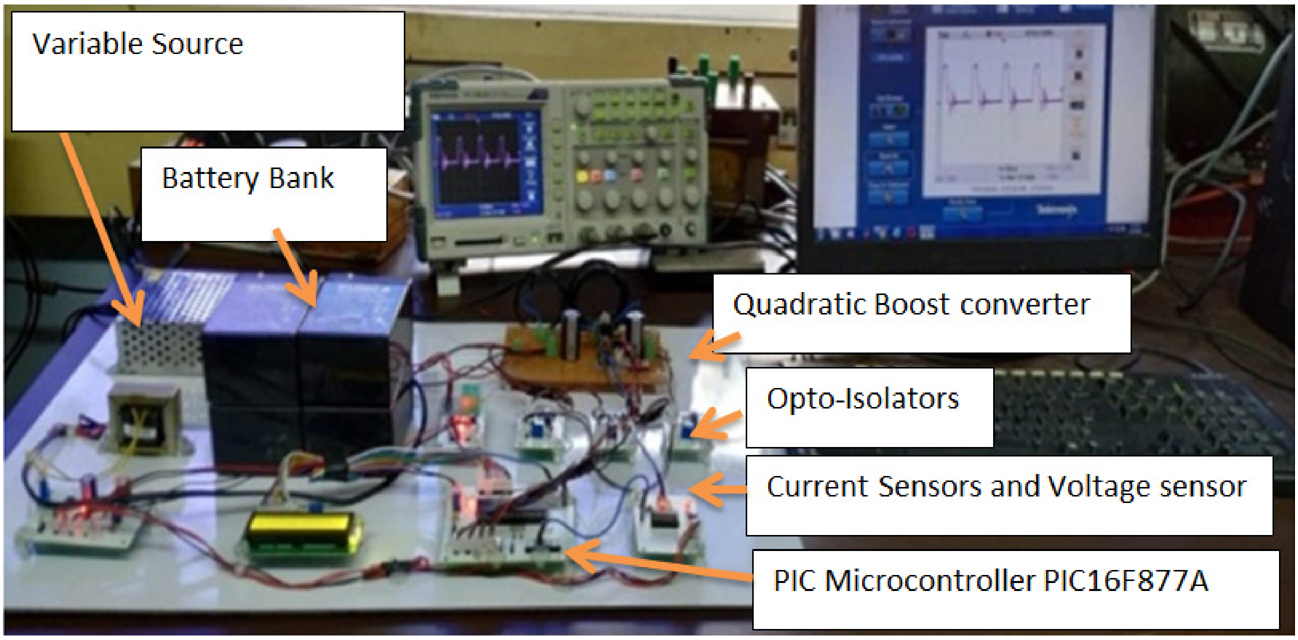

Fig. 10. Experimental prototype.

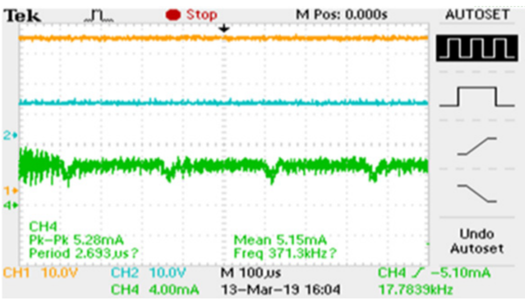

(a)

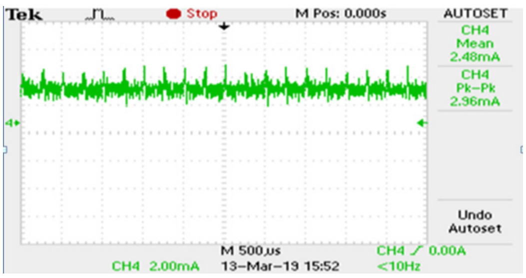

(b)

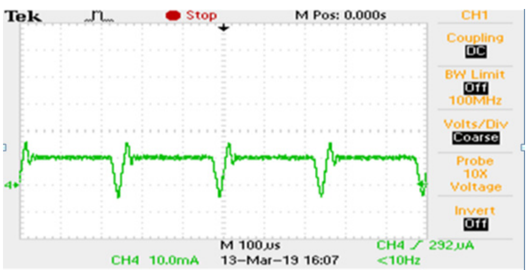

(c)

Fig. 11. Waveforms during discharging of battery (a) Input/Output voltage and battery current (b) Inductor current, I_{L1} (c) Inductor current, I_{L2}.

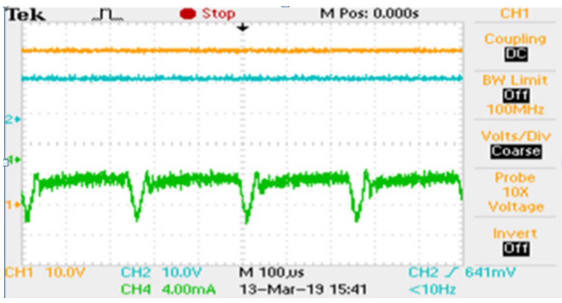

(a)

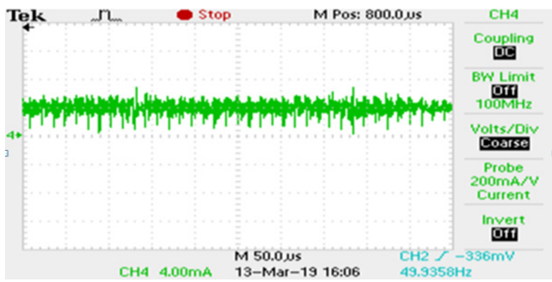

(b)

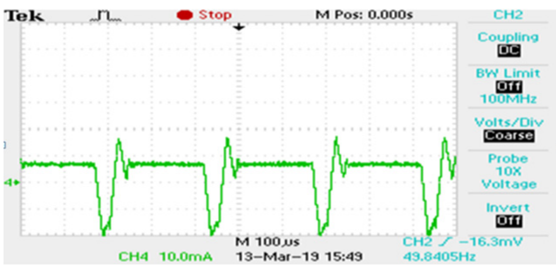

(c)

Fig. 12. Waveforms during charging of battery (a) Input/Output voltage and battery current (b) Inductor current, I_{L1} (c) Inductor current, I_{L2}.

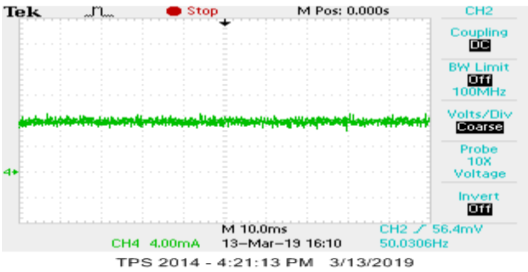

Fig. 13. Load Current of converter.

Now battery is in discharging state. In this state battery voltage stands at 23 V and battery current shown is positive in magnitude. However, embedded C coding in the PIC microcontroller maintains output voltage V_0 at 50V by implementing the algorithm of PI controller. In the other case Figure.12(b) depicts inductor current i_{L1} of 2mA and Figure.12(c) depicts inductor current i_{L2} of 10mA. Figure 16(a) shows input voltage V_{in}, output voltage V_{out} and battery current I_{bat}. Now battery is in charging state; this happens when input voltage is raised to 14 V. In this instant, battery voltage is at 25.5 V and battery current shown is negative in magnitude and change in the direction of battery current is indicated. Figure.12(b) depicts inductor current i_{L1} of 4mA and Figure.12(c) depicts inductor current i_{L2} of 7.5mA. In this case also output power is maintained at 50V by PIC microcontroller. Figure 13 shows the load current of 7.5 mA.

This changeover situation could be clearly understood by comparing inductor currents i_{L1} and i_{L2}. When a transition happens from discharging to charging state inductor current i_{L1} increases from 2mA to 4mA which obviously proves increased value of PV power. Similarly on comparing the waveform of i_{L2}, inductor current has decreased from 10mA to 7.5mA, obviously proving the concept that discharging battery current (i.e.) as transition happens from discharging to charging in battery, the extra battery current that was flowing in inductor i_{L2} is withdrawn and could be understood as its magnitude decreases from 10mA to 7.5mA.

The proposed PV system can be used in solar powered telecommunication systems where it is essential to maintain power and voltage at a constant value in a steady manner. One more application of this converter is in DC nanogrid. This converter is a suitable converter that balances power between low voltage PV panel and DC bus of nanogrid. Due to disparity of DC bus voltage levels found in literature DC bus is maintained at 48V [Moussa et al., 2019]. DC Nano grid is considered superior to AC Nano grid [Rahman et al., 2019]as in conventional AC Nano grid, PV system grieves from power loss caused with power conversion stage from DC-AC-DC as most typical home loads are DC. [Luo et al., 2019]. To get more advantages from proposed design, it could be extended to partial Nano grids as partial Nano grids are more feasible than full DC Nano grids. Battery swapping [Ban et al., 2019] concept suggested to supply fully charged batteries from nanogrid to a battery swapping regional Electric Vehicle station helps creating extended employment opportunities. Table. 4 shows comparison made between existing and proposed converter. Comparison shows that the proposed converter is a suitable converter for low power DC nano-grids.

Table. 4 Comparison between existing and proposed PV system in DC Nano grids.

Topology Parameter	**Ge et al, 2014**	**Proposed converter**	**Metwally et al., 2019**
Number of converters	Single converter with integrated battery storage	Single converter with integrated battery storage	Two converters: One converter to supply power from PV panel to load and second converter that charges PV excess power and discharges power to load during insufficient PV power generation.
Cost saving	More cost saving	More cost saving	Less cost saving
Output power	AC power (needs again to be converted to DC for DC residential loads	DC power	DC power
Compatibility with DC Nano grid	Less compatible	More compatible	More compatible
Possibility of extension of employment in E2V (Future aspect)	Poor	Good	moderate

6. CONCLUSION

QBC integrated with energy storage is discussed in this paper, holds advantages like high voltage gain, maintenance of constant output power at load, simple and cost effective compared to the use of bi-directional converters for energy storage. Battery connected in parallel with the capacitor of the QBC smoothens power fluctuations transmitted from panel to load side. This proposed converter also precludes the use of bi-directional converters for energy storage. Design of inductor and capacitor operates the converter at continuous conduction mode. The linear averaged model is derived to obtain the transient behaviour of proposed converter. This converter exhibits fourth order characteristic behaviour. Current mode control is implemented with fast tracking inner loop and outer voltage loop. PI controller values selected ensure robust stability and output voltage regulation. Proposed converter is a suitable converter that can be embedded in PV powered telecommunication system and goes well in PV powered Residential application that embeds DC grids. The experimental verification of converter that is proposed has been made with 100 W prototype and tested to validate the theoretical and simulation results.

7. FUTURE SCOPE

The work is planned to be extended for high power handling applications like Electric vehicle charging stations.

REFERENCES

Ban, M., Yu, J., Shahidehpour, M. et al. (2019). Optimal sizing of PV and battery-based energy storage in an off-grid nan grid supplying batteries to a battery swapping station. *J. Mod. Power Syst. Clean Energy,* Vol.7, pp.309–320.

Beltran, H., Bilbao, E., Belenguer, E., Etxeberria-Otadui, I. and Rodriguez, P. (2013). Evaluation of Storage Energy Requirements for Constant Production in PV Power Plants. *IEEE Transactions on Industrial Electronics*, Vol.60, No.3, pp.1225-1234.

Bortolini, M., Gamberi, M. and Graziani, A. (2014). Technical and economic design of photovoltaic and battery energy storage system. *Energy Conversion and Management,* Vol.86, pp.81-92.

Child, M., Kemfert, C., Bogdanov, D. and Breyer, C. (2019). Flexible electricity generation, grid exchange and storage for the transition to a 100% renewable energy system in Europe. *Renewable energy*, Vol.139, pp.80-101.

Dong, D., Cvetkovic, I., Boroyevich, D., Zhang, W., Wang, R. and Mattavelli, P. (2012). Grid-interface bidirectional converter for residential DC distribution systems—Part one: High-density two-stage topology. *IEEE Transactions on Power Electronics*, Vol.28, No.4, pp.1655-1666.

Ge, B., Peng, F. Z., Abu-Rub, H., Ferreira, F. J. T. E. and de Almeida, A. T. (2014). Novel Energy Stored Single-Stage Photovoltaic Power System with Constant DC-Link Peak Voltage. *IEEE Transactions on Sustainable Energy,* Vol.5, No.1, pp.28-36.

Ge, B., Abu-Rub, H., Peng, F.Z., Lei, Q., De Almeida, A.T., Ferreira, F.J., Sun, D. and Liu, Y. (2012). An energy-stored quasi-Z-source inverter for application to photovoltaic power system. *IEEE transactions on industrial electronics*, Vol.60, No.10, pp.4468-4481.

Ge, B., Liu, Y., Abu-Rub, H. and Peng, F. Z. (2018). State-of-Charge Balancing Control for a Battery-Energy-Stored Quasi-Z-Source Cascaded-Multilevel-Inverter-Based Photovoltaic Power System. *IEEE Transactions on Industrial Electronics,* Vol.65, No.3, pp.2268-2279.

Gulagi, A., Bogdanov, D. and Breyer, C. (2018). The role of storage technologies in energy transition pathways towards achieving a fully sustainable energy system for India. *Journal of Energy Storage*, Vol.17, pp.525-539.

Haroun, R., Nassary, M., Orabi, M. and Aroudi, A. E. (2019) Analysis, Design and Simulation of a DC Photovoltaic Microgrid with Electric Vehicle Charging Capability. *IEEE Conference on Power Electronics and Renewable Energy (CPERE), Aswan City, Egypt*, pp.222-227.

Jadhav, S., Devdas, N., Nisar, S. and Bajpai, V., 2018, January. Bidirectional DC-DC converter in solar PV system for battery charging application. *In 2018 International Conference on Smart City and Emerging Technology (ICSCET)* pp. 1-). IEEE.

Jagadish Kumar Patra, H.M., Tania, D.E. and Arunkumar, G. (2016) A Review on Advancements in DC Micro grid Technology. *Proc. Today*, Vol.9, pp.1265–1279.

Kroposki, B., *et al.* (2017). Achieving a 100% Renewable Grid: Operating Electric Power Systems with Extremely High Levels of Variable Renewable Energy. *IEEE Power and Energy Magazine*, Vol.15, No.2, pp.61-73.

Li, W., Mou, X., Zhou, Y. and Marnay, C. (2012). On voltage standards for DC home microgrids energized by distributed sources. *In Proceedings of the 7th International Power Electronics and Motion Control Conference (IPEMC), Harbin, China*, Vol.3, pp.2282–2286.

Leyva-Ramos, J., Ortiz-Lopez, M.G., Diaz-Saldierna, L.H. and Morales-Saldana, J.A., (2009). Switching regulator using a quadratic boost converter for wide DC conversion ratios. *IET Power Electronics*, 2(5), pp.605-613.

Leyva-Ramos, J., Mota-Varona, R., Ortiz-Lopez, M. G., Diaz-Saldierna, L. H. and Langarica-Cordoba, D. (2017). Control Strategy of a Quadratic Boost Converter with Voltage Multiplier Cell for High-Voltage Gain. *IEEE Journal of Emerging and Selected Topics in Power Electronics*, Vol.5, No.4, pp.1761-1770.

Liang, W., Liu, Y., Ge, B., Abu-Rub, H., Balog, R.S. and Xue, Y. (2017). Double-line-frequency ripple model, analysis, and impedance design for energy-stored single-phase quasi-Z-source photovoltaic system. *IEEE Transactions on Industrial Electronics*, Vol.65, No.4, pp.3198-3209.

Liu, Y., Ge, B., Abu-Rub, H. and Peng, F. Z. (2013). Control System Design of Battery-Assisted Quasi-Z-Source Inverter for Grid-Tie Photovoltaic Power Generation. *IEEE Transactions on Sustainable Energy,* Vol.4, No.4, pp.994-1001.

Liu, Y., Ge, B., Abu-Rub, H. and Peng, F.Z. (2014). Modelling and controller design of quasi-Z-source inverter with battery-based photovoltaic power system. *IET Power Electronics*, Vol.7, No.7, pp.1665-1674.

Lopes, L.A.C. and Lienhardt, A.M., (2003). A simplified nonlinear power source for simulating PV panels. *In IEEE 34th Annual Conference on Power Electronics Specialist, 2003. PESC'03.* Vol. 4, pp. 1729-1734. IEEE.

Lopes, R.A., Martins, J., Aelenei, D. and Lima, C.P. (2016). A cooperative net zero energy community to improve load matching. *Renewable Energy*, Vol.93, pp.1-13.

Luo, Y. Z. and Lie, T. T. (2019). Energy Savings Using Direct Current (DC) from Photovoltaic (PV) System in a Residential Home. *IEEE Innovative Smart Grid Technologies - Asia (ISGT Asia), Chengdu, China*, pp.2467-2471.

Kavya Santhoshi B. and Mohana Sundaram K. (2020) A Cost-Effective PV-Based Single-Stage Conversion System for Power Backup. In: Saini H., Srinivas T., Vinod Kumar D., Chandragupta Mauryan K. (eds) Innovations in Electrical and Electronics Engineering. *Lecture Notes in Electrical Engineering*, Vol.626. Springer, Singapore

Khajesalehi, J., Sheshyekani, K., Hamzeh, M. and Afjei, E. (2015). High-performance hybrid photovoltaic-battery system based on quasi-Z-source inverter: application in microgrids. *IET Generation, Transmission & Distribution*, Vol.9, No.10, pp.895-902.

Manandhar, U., Ukil, A. and Jonathan, T.K.K. (2015). Efficiency comparison of DC and AC microgrid. In Proceedings of the IEEE PES Innovative Smart Grid Technologies *Conference—Asia (ISGT Asia), Bangkok, Thailand*, Vol.3, No.6, pp.1–6.

Metwally, S. H., Zhang, X., Ali, S. and Krishnamoorthy, H. S. (2019). Solar PV and BESS based Home Energy System," *2019 IEEE Texas Power and Energy Conference (TPEC), College Station, TX, USA*, pp.1-6.

Moussa, S., Ghorbal, M. J. B. and Slama-Belkhodja, I. (2019). Bus voltage level choice for standalone residential DC nanogrid. *Sustainable Cities and Society,* Vol.46, pp.101431

Moumouni, Y., Baghzouz, Y. and Boehm, R.F. (2014). Power "smoothing" of a commercial-size photovoltaic system by an energy storage system. *In 2014 16th International Conference on Harmonics and Quality of Power (ICHQP) IEEE*, pp.640-644.

Nottrott, A., Kleissl, J. and Washom, B. (2013). Energy dispatch schedule optimization and cost benefit analysis for grid-connected, photovoltaic-battery storage systems. *Renewable Energy*, Vol.55, pp.230-240.

Nyholm, E., Goop, J., Odenberger, M. and Johnsson, F. (2016). Solar photovoltaic-battery systems in Swedish households–Self-consumption and self-sufficiency. *Applied energy*, Vol.183, pp.148-159.

Rahman, F. A., James, R., Jose, S., Ahmed, S., Mohammed M. S. A. and Kunju, K. B. (2019). Solar DC Homes: Energy for All. *TENCON 2019 - 2019 IEEE Region 10 Conference (TENCON), Kochi, India*, pp.2428-2432.

Ren, Z., Grozev, G. and Higgins, A. (2016). Modelling impact of PV battery systems on energy consumption and bill savings of Australian houses under alternative tariff structures. *Renewable Energy*, Vol.89, pp.317-330.

Rodriguez-Diaz, E., Savaghebi, M., Vasquez, J.C. and Guerrero, J.M., (2015). An overview of low voltage DC distribution systems for residential applications. *In 2015 IEEE 5th International Conference on Consumer Electronics-Berlin (ICCE-Berlin)* pp. 318-322. IEEE.

Silveira, J. P. C., Neto, P. J. d. S., de Paula, M. V., de Souza, R. R., Barros, T. A. d. S. and Filho, E. R. (2018). Evaluation of Bidirectional DC-DC Converter Topologies for Voltage Regulation in Hybrid Microgrids with Photovoltaic and Battery Technologies. *13th IEEE International Conference on Industry Applications (INDUSCON), São Paulo, Brazil,* pp.215-221.

Starke, M., Tolbert, L.M. and Ozpineci, B. AC vs. DC Distribution: A loss comparison. (2008). *In Proceedings of the IEEE/PES Transmission and Distribution Conference and Exposition, Chicago, IL, USA,* pp. 1–7.

Vieira, F.M., Moura, P.S. and de Almeida, A.T. (2017). Energy storage system for self-consumption of photovoltaic energy in residential zero energy buildings. *Renewable Energy*, Vol.103, pp.308-320.

Wunder, B., Ott, L., Szpek, M., Boeke, U. and Weiss, R., (2014), September. Energy efficient DC-grids for commercial buildings. In 2014 IEEE 36th International Telecommunications Energy Conference (INTELEC) pp. 1-8. IEEE.